UNIZIK JOURNAL OF ENGINEERING AND APPLIED SCIENCES (UJEAS)

Research Article

Kinetics and Thermodynamics of Biolubricant Production from Lard Oil Using EG and TMP

R.S. Odera, O.D. Onukwuli, Victor E. Ojukwu and E.E. Oharie

Special Issue
A Themed Issue in Honour of Professor Onukwuli Okechukwu Dominic (FAS).

This special issue is dedicated to Professor Onukwuli Okechukwu Dominic (FAS), marking his retirement and celebrating a remarkable career. His legacy of exemplary scholarship, mentorship, and commitment to advancing knowledge is commemorated in this collection of works.

Edited by
Chinonso Hubert Achebe PhD.
Christian Emeka Okafor PhD.

UJEAS

UNIZIK JOURNAL OF ENGINEERING AND APPLIED SCIENCES

UNIZIK Journal of Engineering and Applied Sciences 4(1), March (2025), 1697-1705
Journal homepage: https://journals.unizik.edu.ng/index.php/ujeas
PRINT ISSN: 2992-4383 || ONLINE ISSN: 2992-4391

Kinetics and Thermodynamics of Biolubricant Production from Lard Oil Using EG and TMP

R.S. Odera[1], O.D. Onukwuli[1] , Victor E. Ojukwu[1*] and E.E. Oharie[2]
[1]Department of Chemical Engineering, Nnamdi Azikiwe University, Awka, Anambra State, Nigeria
[2]Dangote Cement Plant Plc, Obajana, Kogi State, Nigeria.
*Corresponding author's email address: ve.ojukwu@unizik.edu.ng

Abstract
This study presents the kinetics and thermodynamics correlation of biolubricants derived from lard oil-based stock using ethylene glycol (EG) and trimethylolpropane (TMP). Kinetic data fitting for $LOBL_{EG}$ to both first and second-order kinetic rate laws showed that the R^2 value for the first-order model were higher than that for the second-order model. This implies that the kinetic data for $LOBL_{EG}$ follows a simpler kinetic behavior that can be easily modeled. In contrast, in $LOBL_{TMP}$, the R^2 value of the second-order model was higher, indicating a better fit. In terms of thermodynamics, it was observed that the reaction process for $LOBL_{EG}$ was endothermic, with an ΔH value of 54.9 kJ/mol, while for $LOBL_{TMP}$, it was exothermic with an ΔH value of -91.5 kJ/mol. Furthermore, the kinetic data for $LOBL_{EG}$ did not align with the Michaelis-Menten rate law, as indicated by an R^2 value of 0.81, in contrast to the R^2 value of 0.95 obtained for $LOBL_{TMP}$ which agrees closely with the kinetic reaction to produce $LOBL_{TMP}$. These findings suggest that $LOBL_{TMP}$ exhibits a more temperature-driven reaction rate than $LOBL_{EG}$, while the latter showed a higher energy-saving capacity due to lower activation energy. Thus, both routes offer means through which environmentally friendly lubricants can be produced and data provided here could be used to design reactors that can produce biolubricants.

Keywords: biolubricant; lard base-oil; ethylene glycol (EG); trimethylolpropane (TMP); kinetic; thermodynamics; ethylene glycol biolubricant ($LOBL_{EG}$); trimethylolpropane biolubricant ($LOBL_{TMP}$)

Introduction

Around the world today, the inundation of human-induced activities has led to unprecedented energy requirements which has necessitated global warming and ozone-layer depletion. As fossil fuel is the major source of energy in our world, it has become grossly inefficient to meet the spike. Fossil fuels are not only a deleterious energy source but petrochemicals and lubricants add to the mix with impacts ranging from complete loss usage to major accidents (Alsultan et al., 2021). It is also very interesting to know that out of the over 30 million tons of lubricants produced worldwide about 95% is linked to fossil fuel thus necessitating the birth of a renewable, sustainable and cheap energy source called biofuel (Rudnick and Bartz, 2020, Alsultan et al., 2021, Cecilia et al., 2020). These have become the favourites as they have helped in curtailing the global emergency called global warming and its attendant consequences (Rudnick and Bartz, 2020). Lubricants can produced conventionally from minerals or petroleum which can be applied to a wide range of machinery in the mechanical industries because of their effective lubricating properties (Resul et al., 2011).

Although this offers good quality in application, our environment pays heavily due to attendant deleterious effects on the environment. Oils from both plants and animals can be a source of huge relief for the environment although at an early stage of utility offer better advantages ranging from high viscosity to low coefficient of friction (Resul et al., 2011, Ocholi et al., 2018). They are also in high demand due to their readily availability, amenable qualities, and eco-friendliness (Ocholi et al., 2018). Biolubricants remain the sure alternative for synthetic biolubricants for several reasons; the processes used in the production are green, non-toxic and renewable, they are affordable and the biolubricant can be safely disposed of into the environment without fears as the conditions for environmentally-friendly products are met (Resul et al., 2011, Owuna et al., 2020). Many routes exist for the production of biolubricant

but one of the most widely used is the double transesterification approach where the vegetable oil or animal oil is transformed first to biodiesel (in the presence of alcohol) and then to biolubricant (in the presence of higher alcohol) (Hussein et al., 2021). Despite the advantages of biolubricants they equally have some disadvantages which may include; thermal stability over a narrow range of temperatures which can be overcome by chemical modification of fatty acids in the base oil or fat (Owuna et al., 2020), rapid oxidation which can necessitate the changing of the biolubricant which can overcome using antioxidants in other to elongate their service life (Cecilia et al., 2020), poor viscosity index and low-temperature properties can be overcome via chemical modifications (Salih and Salimon, 2021, Menkiti et al., 2017).

Lots of work has used vegetable oil and has equally focused on the yield of the biolubricant in the presence of competing factors and also the kinetics and thermodynamics of oil-base biolubricants (Menkiti et al., 2017, Ocholi et al., 2018, Rudnick and Bartz, 2020, Resul et al., 2011). To the best of our knowledge, only very few have reported the kinetics and thermodynamics of lard oil-based lubricant comparatively. In the study of Menkiti et al, (Menkiti et al., 2017), which focused on the production of environmentally friendly lubricant basestock from jatropha curcas specie seed oil, Gibb's free energy indicated a spontaneous reaction having a second order rate constant of $1.00e^{-01}$(%wt/wtmin)C^{-1} and a kinetic energy of 13.57kj/mol. Also in their work, Aziz et al (Aziz et al., 2020), discovered that the transesterification reaction of palm oil-based methyl trimethylolpropane (TMP) data fitted with the second-order reversible reaction kinetics with the reaction rate constant in the range of 0.01-0.63 $[(w/w)(min)]^{-1}$. This work focused on the comparative study of the kinetics and thermodynamics of biolubricant production from lard oil base stock via ethylene glycol (EG) and trimethylolpropane (TMP).

2.0 Materials and methods

2.1 Materials

The lard oil was obtained from Onitsha's local market. The reagents were provided by Eddyson International and were all of analytical grade. The materials used were sodium hydroxide, anhydrous methanol, potassium hydroxide, sodium methoxide (30% in methanol), tetraoxosulphate (IV) acid, hydrochloric acid, ethylene glycol (EG) isopropyl alcohol, phenolphthalein indicator and trimethylolpropane.

2.2 Synthesis and characterization of lard oil from Pure pig fat

A rendering technique was used to obtain the lard oil from the raw pig fact. The raw pig fat was shredded into tiny pieces placed in a clean beaker and boiled on a water birth for thirty minutes. After this, a clear mixture of lard oil and crackling was formed. The synthesized lard oil was separated from the cracklings by the process of sifting. The extracted oil was placed in a jar and corked. The result of the characterization of the raw lard oil is shown in the table below in Table 1 which confirms that it is suitable for biolubricant production (Hamnas et al., 2023)

Table 1: Result of characterization of Lard oil

Parameters	Values
Saponification value	201
Free fatty acid	0.82
Flash point	205
Iodine value	61
Mean molecular weight (g mol^{-1})	857.34
moisture content (wt %)	0.01
Kinematic viscosity	44

2.3 Pretreatment of the Lard Oil (LO)

100g of samples (oil) are measured and placed in a round bottom flask with 20% w/w methanol and 5% w/w tetraoxosulphate (VI). In a water bath, the acid-methanol mixture together with the oil sample was heated to 60°C. After 60 minutes, the sample was extracted using a picking pipette and titrated against a 0.1M NaOH solution to obtain the acid value of the sample. After that, the FFA is calculated by dividing the Acid value by 2. The titration was done 4 times for 240 minutes at 60-minute intervals.

2.4 Synthesis of lard methyl ester (LME)

100 mL of lard oil sample was placed in 250 mL conical flasks and boiled on a magnetic stir hot plate to 60ºC. The potassium hydroxide was then dissolved in a shaken 100ml beaker which contains 22ml of 1%wt (10g) anhydrous methanol (Ocholi et al., 2018). This was followed by the combination of potassium hydroxide solution with a 1:6 oil-to-methanol ratio with a warm 100-lard oil sample. The methanol was used in excess to ensure the right ratio for methyl ester production as was also adopted by Menkiti et al (Menkiti et al., 2017). The solution was then effectively stirred for 60 minutes at 700 revolutions per minute with a magnetic stirrer. To ensure proper concentration, the solution was placed in a separating funnel for 24 hours. At the end of the sedimentation procedure, the top layer (methyl ester) was poured into a beaker and washed with warm distilled water. This process is used to get rid of unreacted methanol, catalyst, glycerol, and other extraneous materials. The moisture in the methyl ester sample was removed in an oven set to 60ºC. Lastly, the funnel's bottom was used to collect the glycerol-containing lower layer. (Egbuna et al., 2021).

2.5 Synthesis of lard biolubricant

The resulting methyl ester was combined with ethylene glycol to form an ethylene glycol ester or lard oil lubricant. The ethylene glycol was poured into a 100ml beaker and boiled to 110ºC on a hot plate for 15 minutes before being cooled. This is done to eliminate all moisture from the ethylene glycol sample. The sodium methoxide catalyst was produced by dissolving about 30g of pure sodium metal in 100g of anhydrous methanol. For 5 minutes, the cooled ethylene glycol sample was intensively mixed with 0.8%wt of the generated sodium methoxide catalyst (Encinar et al., 2020) . Following that, a methyl ester sample was added in excess to the sodium methoxide/ethylene glycol mixture at a mole ratio of 4:1. The solution was then intensively agitated for 3 hours using a magnetic stir hot plate at a revolution rate of 700 per minute at a reaction temperature of 150ºC to enable effective collision of the reactant.

3.0 Result and Discussion

3.1 Kinetic and thermodynamic studies of the biolubricant products

To determine the optimal kinetic model, a comparison was conducted between trimethylolpropane and ethylene glycol in the second stage transesterification reaction. The reaction pathway is illustrated below:

LOME+TMP ⇌ ME+M (1)

LOME+ME ⇌ DE+M (2)

LOME+DE ⇌ TE+M (3)

Overall reaction:

3LOME+TMP ⇌TE+3M (4)

The provided equation reveals that in the context of this study, DE represents diester, TE stands for trimester, LOME denotes lard oil methyl ester, M represents methanol, and ME represents monoester, while TMP signifies trimethylolpropane. The kinetic analysis was conducted over a period ranging from 44 to 220 minutes. Maintaining a stoichiometric ratio of LOME to TMP at 3:1, TMP was intentionally limiting reactant to carefully control the reaction. LOME was kept in excess to ensure the transesterification proceeded to completion through the forward reaction, even in the face of the reaction's reversibility. To facilitate the forward reaction, constant removal of methanol from the system was implemented, even though the reaction tends to favor high temperatures for optimal progression. Implementing this approach was crucial as it played a vital role in promoting the desired reaction pathway and ensuring the thorough completion of the transesterification process. (Resul et al., 2011). The rate constants, K_{TMP} and K_{EG}, were determined by observing the reduction in trimethylolpropane and ethylene glycol concentrations, respectively. The rates for the first and second-order reactions are represented in Equations 5-8 as follows:

First-order Kinetic model

$$\ln[TMP] = -K_{TMP}\,t + \ln[TMP_0] \quad (5)$$

$$\ln[EG] = -K_{EG}\,t + \ln[EG_0] \quad (6)$$

Second order Kinetic model

$$\left[\frac{1}{TMP}\right] = K_{TMP}t + \left[\frac{1}{TMP_0}\right] \quad (7)$$

$$\left[\frac{1}{EG}\right] = K_{EG}t + \left[\frac{1}{EG_0}\right] \quad (8)$$

[TMP] and [EG] represent the concentrations of trimethylolpropane and ethylene glycol reactants, respectively. [TMPO] and [EGO] denote the initial concentrations of trimethylolpropane and ethylene glycol reactants, respectively. K_{TMP} and K_{EG} stand for the first and second-order rate constants for these reactants. The proposed rate

laws were utilized to fit the generated kinetic data. The idea here is that the data obtained from the biolubricant production has to follow a particular well-known trend when plotted which tells us the type of reaction that took place (first or second order). This model is the relationship between the dependent and independent variable and the data is said to be a good fit if the R^2 value is close to 1 and does not if <1. The kinetic models for the first and second-order kinetics for $LOBL_{TMP}$ and $LOBL_{EG}$ were investigated, and the corresponding R^2 values can be found in Table 1 and Table 2, respectively. For all observed temperatures in $LOBL_{TMP}$, the R^2 values for the second-order kinetic model plots were consistently higher than those of the first-order model (Resul et al., 2011). In the case of $LOBL_{EG}$, the R^2 values for the first-order model were higher than those of the second-order model. Consequently, the best-fit model for $LOBL_{TMP}$ was the second-order kinetic model, while for $LOBL_{EG}$, it was the first-order kinetic model. This is so since the R^2 value for $LOBL_{TMP}$ is 0.967 (for first order) and 0.996 (for second order) and which ever is closer to 1 wins and the same idea was applied to $LOBL_{EG}$ The overall plots depicting the best kinetic models for the rates of the second and first-order kinetics for $LOBL_{EG}$ and $LOBL_{TMP}$ are presented in Figures 1 (a) and (b), respectively.

Upon analyzing these figures, it is evident that the pathway for the production of $LOBL_{TMP}$ followed the second-order rate law mechanism whilst that of $LOBL_{EG}$ followed the first-order mechanism. The rapid depletion of ethylene glycol, the focal point of this study, resulted in a significant escalation in the reaction rate, particularly within the temperature range of 145 to 150°C. The overall second-order rate constant obtained was 4.44×10^{-1} (%wt/wt min ◦C)$^{-1}$ for the synthesis of $LOBL_{TMP}$ while the overall first-order rate constant was given as 6.4×10^{-1} (%wt/wt min ◦C)$^{-1}$ for $LOBL_{EG}$. Menkiti et al (Menkiti et al., 2015) reported that the kinetic investigation of the synthesis of the biolubricant from fluted pumpkin seed oil gave an overall second-order model having a rate constant of 2.05×10^{-1} (%wt/wt min ◦C)$^{-1}$. Gunam et al (bin Gunam Resul, 2012) reported that the production of jatropha biolubricant via sodium methoxide catalyst followed an overall second-order kinetic model with a rate constant of 1.80×10^{-1} (%wt/wt min ◦C)$^{-1}$, while Nurdin (Nurdin et al., 2015) found that the production of jatropha biolubricant using paphiaundulata shell waste catalyst gave an overall second order reaction with a rate constant of $4.27 \times 10^{\wedge-2}$ (%wt/wt min ◦C)$^{-1}$ which are all in reasonable agreement with this work. From the standpoint of extended application, the rate mechanism and rate constants obtained from this work could be utilized in the design of reactor systems that can run the transesterification reaction to verify the extent of biolubricant yield possible.

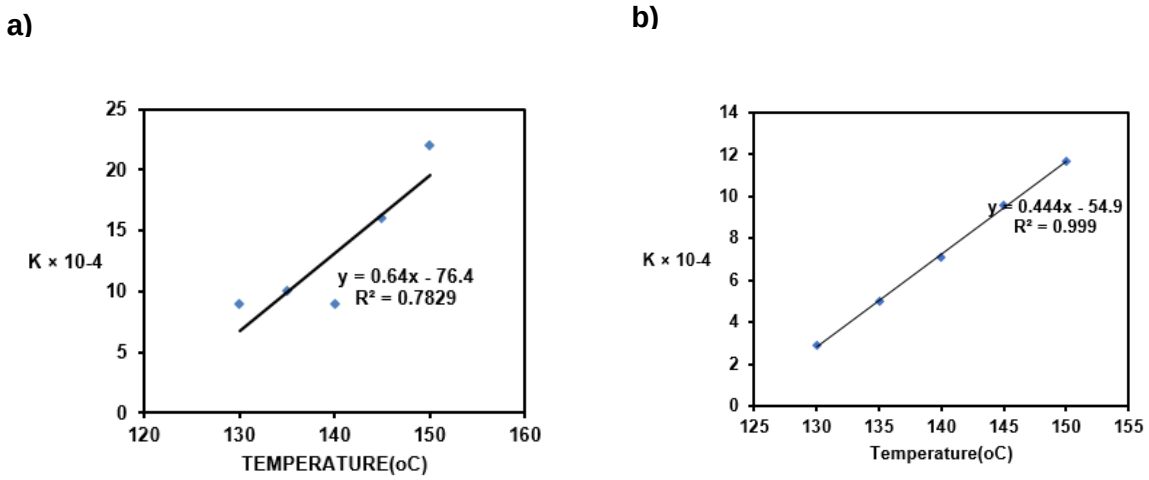

Fig 1. a) Overall second-order kinetics model for the synthesis of $LOBL_{EG}$ at various temperatures b) Overall first-order kinetics model for the synthesis of $LOBL_{TMP}$ at various temperatures.

3.2 Transesterification thermodynamics.

The dependency of the rate constant, k on temperature will fit the Arrhenius equation given below in Eqn 8-9;

$$\log_{10} K = \frac{-EA}{2.303RT} + \log_{10} A \quad (8)$$

$$Slope = \frac{-EA}{2.303R} \quad (9)$$

Here, R represents the gas constant R = 8.314J /K/mol, and T denotes the temperature in Kelvin. The activation energy EA for both TMP and EG lubricant (i.e.$LOBL_{TMP}$ and $LOBL_{EG}$) can be determined from the slope of the plot of $\log_{10}k$ against 1/T, as illustrated in Figures 2 (a) and (b), respectively. Upon analysing the transesterification process, the calculated activation energy for $LOBL_{TMP}$ and $LOBL_{EG}$ was found to be 95.7 kJ/mol and 54.9 kJ/mol, respectively. These values fall below the generally accepted range of 139.3 – 141.8 kJ/mol, indicating that the activation energies observed in this study are comparatively lower than the established standard range. (Aziz et al., 2020). Since a high activation energy implies a very slow reaction rate, a higher activation energy of the $LOBL_{TMP}$ reaction implies a slower reaction when compared with $LOBL_{EG}$ at different temperatures. This may be due to the different reaction mechanisms followed by $LOBL_{TMP}$ and $LOBL_{EG}$, steric effects, and reactant-catalyst interaction as the two were subject to the same operating conditions. As a result, we recorded about 32% and 61% energy-saving on $LOBL_{TMP}$ and $LOBL_{EG}$, respectively. Higher energy-saving recorded on $LOBL_{EG}$ is due to the completion of the reaction as the temperature increased from 140°C to 150°C as compared to $LOBL_{TMP}$. Other researchers have also recorded similar results namely; Menkiti et al (Menkiti et al., 2017) found an activation energy of 13.57kJ/mol for jatropha biolubricant synthesis, Menkiti et al (Menkiti et al., 2015) also found an activation energy of 41.40kJ/mol for fluted pumpkin seed oil while Resul et al (Resul et al., 2012) published an activation energy of 3.94kJ/mol. It is important to note that slight variations in reported activation energy values may arise due to differences in the temperature range considered and the type of catalyst used.

However, it is fundamental to understand that the mechanism of the reaction remains consistent across these variations. Temperature, catalyst, and other reaction conditions do not alter the reaction pathway; instead, they assist in overcoming the energy barrier. Additionally, it is noteworthy that reactions with high activation energy are typically associated with high temperatures, whereas reactions with low activation energy are linked to lower temperatures. This fundamental principle underscores the relationship between activation energy and reaction temperature in chemical processes (Menkiti et al., 2017). Indeed, utilizing heat sources such as microwaves can potentially result in more energy-efficient processes compared to traditional methods like magnetic stir hot plates, however, the energy-saving obtained from this study is higher than that obtained by some researchers, for instance, Aziz et al recorded 49% energy-saving.(Aziz et al., 2020) The thermodynamic properties, including free energy (ΔG), enthalpy change (ΔH), and entropy change, were determined through the application of the second-order reaction constant K (%wt/wt min)$^{-1}$ in the Van't Hoff Equation 10-11.

$$\Delta G^0 = -RT \ln K \quad (10)$$

$$\ln K = \frac{\Delta S^0}{R} - \frac{\Delta H^0}{RT} \quad (11)$$

In the analysis, the natural logarithm of the rate constant LogK was plotted against 1/T (Figure 3 (a) and (b)) to determine the enthalpy change ΔH and entropy change ΔS, as outlined in Tables 1 and 2 for both $LOBL_{TMP}$ and $LOBL_{EG}$ respectively. The positive value of ΔH in Table 1 suggests an endothermic reaction for $LOBL_{EG}$, indicating that the reaction absorbs heat from its surroundings. On the contrary, the negative value of ΔH in Table 2 implies an exothermic reaction for $LOBL_{TMP}$, signifying that this reaction releases heat to its surroundings. This distinction in heat absorption or release explains why $LOBL_{EG}$ achieved lower activation energy, faster reaction completion, and higher energy savings in comparison to its counterpart, $LOBL_{TMP}$. Furthermore, the negative values for the Gibbs free energy ΔG for both $LOBL_{TMP}$ and $LOBL_{EG}$ indicate the thermodynamic feasibility of using both reactants in the transesterification process. The increasing negativity of ΔG as the temperature rises suggests that the transesterification reaction becomes more effective at higher temperatures. However, it's noteworthy that a negative ΔG does not imply the spontaneity of the entire system; it merely shows that the reaction itself is spontaneous. This due to the fact that the reaction system leading to biolubricant production is spontaneous whilst the overall system is equilibrium. Additionally, the positive ΔS values for both $LOBL_{TMP}$ and $LOBL_{EG}$ indicate an increase in the disorder of the system, aligning with observations made by Menkiti et al. (Menkiti et al., 2017). This increase in disorder signifies a trend towards greater randomness or chaos within the system.

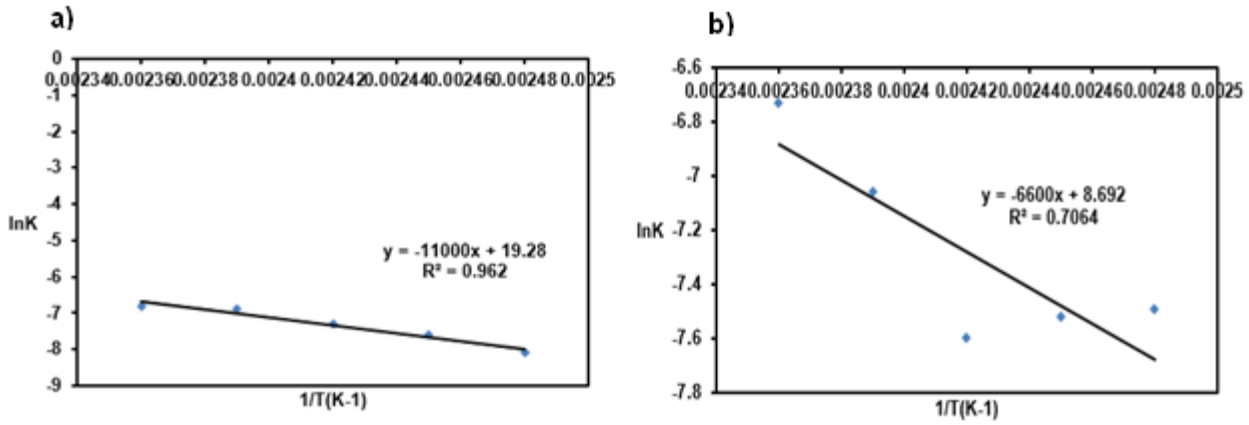

Fig. 2 a): Activation energy plot for the synthesis of $LOBL_{TMP}$ b) Activation energy plot for the synthesis of $LOBL_{EG}$

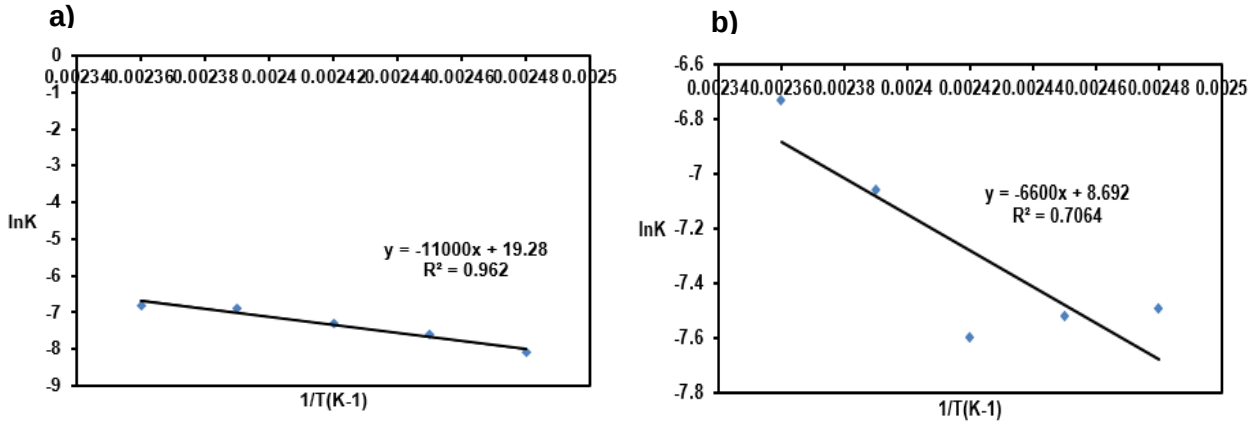

Fig 3 a) Thermodynamic plot for the synthesis of $LOBL_{TMP}$ b) Thermodynamic plot for the synthesis of $LOBL_{EG}$

Table 1: Thermodynamic parameters for $LOBL_{TMP}$ synthesis

T(K)	ΔG(KJ/mol)	ΔS(J/mol K)	ΔH(KJ/mol)
403	-27.3		
408	-25.8		
413	-24.9	160.30	-91.5
418	-24.1		
423	-23.7		

Table 2: Thermodynamic parameters for $LOBL_{EG}$ synthesis

T(K)	ΔG(KJ/mol)	ΔS(J/mol K)	ΔH(KJ/mol)
403	-25		
408	-25.5		
413	-25.8	72.3	54.9
418	-24.5		
423	-23.7		

3.3 Michaelis Menten kinetic model

The equation describes the relationship between reaction velocity and reactant concentration for a system in which the reactant irreversibly combines with the catalyst to form a catalyst-reactant complex. From this complex, a product can be generated. The Michaelis Menten equation is given below as;

$$V = \frac{V_{\max}[S]}{K_M[S]} \quad (11)$$

$$K_M = {}^{1}/_{2V_{max}} \quad (12)$$

In the provided context, V_{max} represents the maximum velocity achieved by the system at maximum reactant concentrations, while K_m (Michaelis constant) signifies the reactant concentration at which the reaction velocity reaches 50% of the maximum velocity V_{max}. Analyzing Table 3 for $LOBL_{TMP}$, it is evident that the maximum velocity V_{max} of the transesterification reaction increases with rising reaction temperature. This observation indicates a higher rate of reaction for $LOBL_{TMP}$ compared to $LOBL_{EG}$. The high regression value R^2 = 0.95 for $LOBL_{TMP}$ suggests that the empirically derived data fits the Michaelis-Menten kinetic model well, defining the kinetic parameters adequately. In contrast, Table 4 for $LOBL_{EG}$ illustrates that there is an almost negligible increment in the maximum velocity V_{max} as the reaction temperature increases. However, an obvious decrease in maximum velocity is observed as the temperature rises from 145°C to 150°C, which could indicate that the transesterification reaction is reaching its endpoint or equilibrium. The average regression value of 0.81 for $LOBL_{EG}$ implies that the derived empirical data does not fit the Michaelis-Menten kinetic model as well as in the case of $LOBL_{TMP}$ which may be because the process was not enzyme catalyzed and proceeded in several stages, unlike the assumption of the Michaelis-Menten model. These findings suggest that $LOBL_{TMP}$ exhibits a more pronounced temperature-dependent reaction rate compared to $LOBL_{EG}$. While the reaction for $LOBL_{TMP}$ fits the Michaelis-Menten model closely, the reaction for $LOBL_{EG}$ may have additional complexities or constraints that deviate from the ideal Michaelis-Menten behaviour.(Cook and Cleland, 2007)

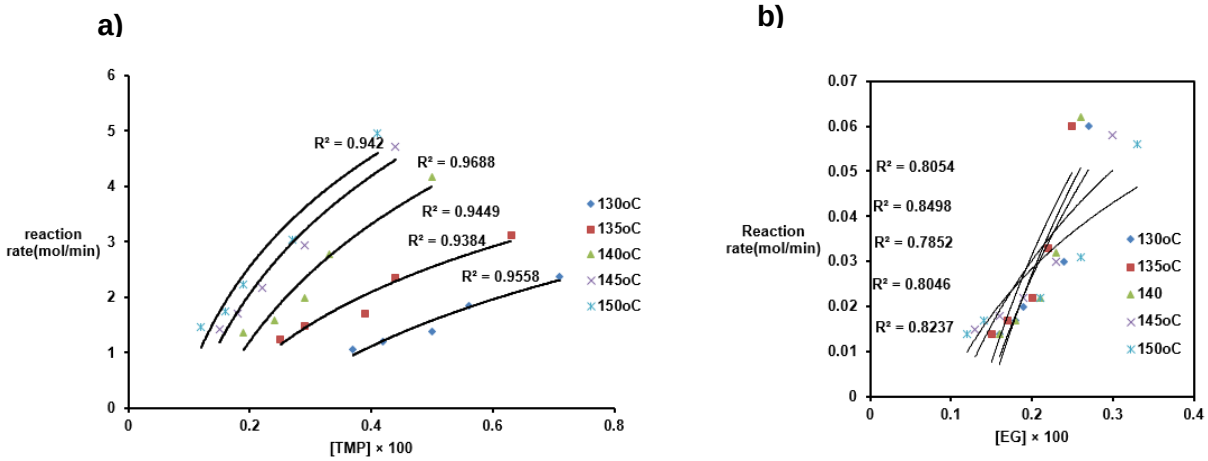

Fig. 4a) A Michaelis-menten kinetic model plot for the synthesis of $LOBL_{TMP}$ b) A Michaelis-Menten kinetic model plot for the synthesis of $LOBL_{EG}$

Table 3: Michaelis menten constants, maximum velocity and regression values at various temperatures for $LOBL_{TMP}$

Temperature	K_m	V_{max}	R^2
130	0.45	2.3	0.96
135	0.3	3	0.94
140	0.27	3.9	0.94
145	0.22	4.4	0.97
150	0.19	4.6	0.94

Table 4: Michaelis menten constants, maximum velocity and regression values at various temperatures for $LOBL_{EG}$

Temperature	K_m	V_{max}	R^2
130	0.17	0.048	0.81
135	0.18	0.050	0.85
140	0.2	0.050	0.79
145	0.2	0.052	0.8
150	0.16	0.049	0.82

4.0. Conclusion

This study constitutes a comparative analysis of the kinetic and thermodynamic properties of biolubricants derived from lard fat base stocks using ethylene glycol ($LOBL_{EG}$) and trimethylolpropane ($LOBL_{TMP}$) as reactants. The results of the kinetic analysis revealed that $LOBL_{EG}$ adhered to the first-order rate law overall, whereas $LOBL_{TMP}$ followed the second-order rate law overall. The distinct heat absorption or release patterns elucidate why $LOBL_{EG}$ exhibited lower activation energy, faster reaction completion, and greater energy efficiency in comparison to $LOBL_{TMP}$. A higher reaction rate implies a lower activation energy, signifying a more economical and efficient process. Although $LOBL_{TMP}$ displayed greater disorderliness, as evidenced by its higher entropy value, it was slower to reach completion compared to its counterpart, $LOBL_{EG}$, which exhibited a lower entropy value. This discrepancy implies that $LOBL_{TMP}$ faced a higher energy barrier, hindering its progress. Furthermore, while the reaction for $LOBL_{TMP}$ closely adhered to the Michaelis-Menten model, the behaviour of the reaction for $LOBL_{EG}$ suggested additional complexities or constraints that deviated from the ideal Michaelis-Menten behaviour. All these findings sum up to the possibility of having biolubricants produced via the animal oil route which opens a promising area for industrial applications. The kinetic models and the rate constant can be used to design reactors for biolubricant production noting that the thermodynamic data assures of the feasibility.

5.0 Recommendation

This work can be further extended to capture other types of animal oils and the process optimized using artificial intelligence to maximize the yield of biolubricants whilst operating within the feasible limits.

Acknowledgments

The authors wish to acknowledge all that were very instrumental to the actualization of this project

Nomenclature

EG- Ethylene glycol
TMP- trimethylolpropane
$LOBL_{EG}$- lard oil-based lubricant from ethylene glycol
$LOBL_{TMP}$- lard oil-based lubricant from trimethylolpropane
K_{EG}- Rate constant for ethylene glycol
K_{TMP}- Rate constant for trimethylolpropane

References

Alsultan, A. G., Asikin-Mijan, N., Ibrahim, Z., Yunus, R., Razali, S. Z., Mansir, N., Islam, A., Seenivasagam, S. & Taufiq-Yap, Y. H. 2021. A short review on catalyst, feedstock, modernised process, current state and challenges on biodiesel production. *Catalysts,* 11**,** 1261.

Aziz, N. A. M., Abd Hamid, H., Yunus, R., Abbas, Z., Omar, R., Rashid, U. & Syam, A. M. 2020. Kinetics and thermodynamics of synthesis of palm oil-based trimethylolpropane triester using microwave irradiation. *Journal of Saudi Chemical Society,* 24**,** 552-566.

Bin Gunam Resul, M. F. M. 2012. *Synthesis of Jatropha Biolubricant Using Sodium Methoxide as Catalyst.* Universiti Putra Malaysia.

Cecilia, J. A., Ballesteros Plata, D., Alves Saboya, R. M., Tavares de Luna, F. M., Cavalcante Jr, C. L. & Rodríguez-Castellón, E. 2020. An overview of the biolubricant production process: Challenges and future perspectives. *Processes,* 8**,** 257.

Cook, P. F. & Cleland, W. W. 2007. *Enzyme kinetics and mechanism*, Garland Science.

Egbuna, S. O., Nwachukwu, U. J., Agu, C. M., Asadu, C. O. & Okolo, B. 2021. Production of biolubricant samples from palm kernel oil using different chemical modification approaches. *Engineering Reports,* 3**,** e12422.

Encinar, J. M., Nogales, S. & González, J. F. J. E. R. 2020. Biodiesel and biolubricant production from different vegetable oils through transesterification. 2**,** e12190.

Hamnas, A., Unnikrishnan, G. J. R. & Reviews, S. E. 2023. Bio-lubricants from vegetable oils: Characterization, modifications, applications and challenges–Review. 182**,** 113413.

Hussein, R. Z., Attia, N. K., Fouad, M. K., ElSheltawy, S. T. J. B. & Bioenergy 2021. Experimental investigation and process simulation of biolubricant production from waste cooking oil. 144**,** 105850.

Menkiti, M., Anaehobi, H., Oyoh, K. & Nnaji, P. 2015. Process optimization and kinetics of biolubricant synthesis from fluted pumpkin seed. *Journal of Chemical Engineering,* 11**,** 1857-7881.

Menkiti, M. C., Ocheje, O. & Agu, C. M. 2017. Production of environmentally adapted lubricant basestock from jatropha curcas specie seed oil. *International Journal of Industrial Chemistry,* 8**,** 133-144.

Nurdin, S., Misebah, F. A., Haron, S. F. & Yunus, R. M. 2015. Transesterification kinetics of jatropha methyl ester and trimethylolpropane for biolubricant synthesis using paphiaundulata shell waste. *Advances in Environmental Biology***,** 35-44.

Ocholi, O., Menkiti, M., Auta, M. & Ezemagu, I. 2018. Optimization of the operating parameters for the extractive synthesis of biolubricant from sesame seed oil via response surface methodology. *Egyptian Journal of Petroleum,* 27**,** 265-275.

Owuna, F., Dabai, M., Sokoto, M., Dangoggo, S., Bagudo, B., Birnin-Yauri, U., Hassan, L., Sada, I., Abubakar, A. & Jibrin, M. 2020. Chemical modification of vegetable oils for the production of biolubricants using trimethylolpropane: A review. *Egyptian Journal of Petroleum,* 29**,** 75-82.

Resul, M. F. M. G., Ghazi, T. I. M. & Idris, A. 2011 Temperature dependence on the synthesis of jatropha biolubricant. IOP Conference Series: Materials Science and Engineering,. IOP Publishing, 012032.

Resul, M. F. M. G., Ghazi, T. I. M. & Idris, A. 2012. Kinetic study of jatropha biolubricant from transesterification of jatropha curcas oil with trimethylolpropane: Effects of temperature. *Industrial Crops and Products,* 38**,** 87-92.

Rudnick, L. R. & Bartz, W. J. 2020. Comparison of synthetic, mineral oil, and bio-based lubricant fluids. *Synthetics, Mineral Oils, and Bio-Based Lubricants.* CRC Press.

Salih, N. & Salimon, J. 2021. A review on eco-friendly green biolubricants from renewable and sustainable plant oil sources. *Biointerface Res. Appl. Chem,* 11**,** 13303-13327.